

Research Article

Impact of Placement of Aminopropyl Triethoxy Silane and Tetraethoxy Silicate on SSBR Chains: Analysis of Rolling Resistance, Wet Grip, and Abrasion Resistance

Majid Hassanabadi, Mohammad Najafi , Sohrab Nikazar, Sadaf Saeedi Garakani, and Ghodrattollah Hashemi Motlagh

Department of Polymer Engineering, School of Chemical Engineering, College of Engineering, University of Tehran, P.O. Box 11155-4563, Tehran, Iran

Correspondence should be addressed to Mohammad Najafi; najafi.m@ut.ac.ir

Received 30 December 2021; Accepted 10 March 2022; Published 5 April 2022

Academic Editor: Adam Kiersnowski

Copyright © 2022 Majid Hassanabadi et al. This is an open access article distributed under the Creative Commons Attribution License, which permits unrestricted use, distribution, and reproduction in any medium, provided the original work is properly cited.

Solution styrene-butadiene rubber (SBR) and silica filler have attracted a significant attention because of their superior properties in cured rubber mixtures used in automobile tire industry. One of the challenges ahead of using these materials is the hard dispersion of silica with its polar surface in SBR nonpolar rubber. In the present study, the synthesis of styrene-butadiene rubber by solution polymerization method with polymer chain modification using copolymer functionalization was performed. For this purpose, two materials, namely, aminopropyl triethoxy silane (APTES) and tetraethoxy silicate (TEOS), were employed to improve the silica dispersion in the mixture. The results of postsynthesis structural tests show the successful placement of functional groups on the polymer chain. The results of mechanical, dynamic, and imaging analyses of the cured mixtures showed an improvement in the APTES-containing samples rolling resistance, wet surface grip, and abrasion resistance by 39%, 18%, and 17%, respectively, due to having stronger physical and chemical bonds with silica and also the usage of end agents in the polymer chain. The samples containing TEOS had also better results than the conventional SBR rubber. In addition, a sample containing emulsion styrene-butadiene rubber was prepared to compare its properties with those of the solution SBR. Another SBR sample containing silane coupling agent was also prepared to investigate its performance compared to that of the agents placed on the polymer chain. The abrasion resistance, rolling resistance, and wet grip of the coupling agent containing sample showed 2%, 10%, and 30% improvement, respectively, which were very close to those of the sample containing the TEOS agent. In this work, various techniques including, rheometry, wear, rolling, hardness, bound rubber content, dynamic mechanical thermal analysis (DMTA), and field emission scanning electron microscopy (FE-SEM) were employed to analyze the synthesized rubber.

1. Introduction

Polymeric nanocomposite materials are attractive materials with wide areas of applications which add to their attraction day by day. The potential applications of these materials include drug delivery, batteries and electrolytes, catalysts, automotive industry, thermal insulation, water treatments, sensors, etc. [1–8]. Due to various demands on the characterization of these materials upon application, different characterization tests such as Fourier transform infrared, nuclear

magnetic resonance, chromatography, electronic microscopy, X-ray diffraction, rheometry, thermal analyses, and various mechanical characterization have to be taken into consideration [9, 10]. There is no doubt that imaging the nowadays world without rubbery goods is almost impossible. They have found their places in our daily life from passenger car and truck tires to footwear, flooring materials, washer sealants, etc.

Normally, elastomers suffer from low wear resistance which is one of the most important aspects of the rubbers

as they are always subject to detachments and stresses. In order to address this problem, it is needed to reinforce the rubber and reduce material loss. The best and most successful effort for this purpose is a filler introduction, like carbon black [11], graphene [12], and silica [13]. Unlike carbon black, the silica surface is polar and not naturally compatible with nonpolar hydrocarbon elastomers. Lack of proper interaction between the filler and the rubber usually results in lower properties compared to a carbon black-filled rubber. A common way to overcome this problem is to use silane coupling agents, which bond silica surface to polymer chains. An alternative is to place the functional groups such as bis(3-triethoxysilyl propyl)tetrasulfide (TESPT3) on the polymer chains. TESPT3 (shown in Figure 1) or Si69 is the most common and popular coupling agent used in the rubber industry [12, 14–19].

A study was conducted by Padenko et al. [20] to investigate the effect of silanized silica particles on mechanical and abrasive wear properties of the peroxide-cured hydrogenated acrylonitrile butadiene rubber (HNBR) with a Shore A hardness similar to that of the compounds containing untreated silica and carbon black. Payne effect studies confirmed the least filler–filler network formation in the composites containing treated silica which was the result of a well dispersion caused by the in situ silanization of silica with vinyltrimethoxysilane; however, the carbon black still showed higher wear resistance. Si69 is able to make condensation reaction with silanol groups on silica surface. Dohi and Horiiuchi [21] studied the mixing temperature effect on the efficiency of the reactions between TESPT and silica and showed that the reaction rate is higher at a temperature of around 150°C.

For styrene-butadiene rubber, a rubber with one of the highest production rates in the world, the functionalization of SBR chain-ends through anionic polymerization has been considered as the best approach. Solution polymerized styrene-butadiene rubber has so many advantages such as higher ability to control microstructure and molecular weight properties of the copolymer, better abrasion resistance, and lower heat generation. Moreover, the anionic polymerization nature provides the attractive advantage of chain modification capability. Using this approach guarantees the uniform dispersion of all functional agents into the matrix in contrast to the method of silane coupling agents' addition [13, 22–24]. Lin et al. [15] reported a less developed filler–filler network in a functionalized SBR with both tin (Sn) and tetraethyl orthosilicate (TEOS) as a result of the enhanced polymer–filler interaction.

In the present work, following the last approach, 3-(aminopropyl)triethoxysilane (APTES) as the functionalization agent was used in order to decrease the hydrophobicity of SBR. Another functionalized synthetic styrene butadiene rubber (SSBR) was prepared using tetraethyl orthosilicate (TEOS). The TEOS (Figure 2(a)) and APTES (Figure 2(b)) were used for the functionalization of polymer chains. The TEOS with four identical branches of ethoxy sticks to the chain when one of the branches is removed, and the other branches react with it during mixing with silica. The APTES with three ethoxy branches and one amine branch sticks to

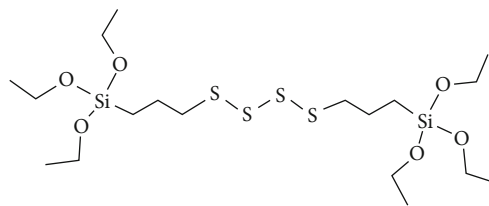


FIGURE 1: The chemical structure of silane coupling agent Si69.

the chain by removing one ethoxy branch and attaches to the silica using the remaining ethoxy and amine branches.

Liu et al. [22] synthesized a solution styrene butadiene rubber using anionic polymerization with alkoxy silane on both sides of the chain by a lithium initiator and reported that by modifying this new structure, chemical bonds were created instead of the usual physical bonds between the rubber and silica matrices. It is concluded that the modified rubber had better performance in terms of rolling resistance and resistance on wet surfaces compared to the rubbers prepared using conventional methods, which indicates the application of this rubber in green tires. In this work, the dynamic mechanical thermal analysis (DMTA) was performed to determine the $\tan(\delta)$ values for the mixtures. At a temperature of 0 and 60°C, the values of 0.4 and 0.06, respectively, for the modified sample and 0.2 and 0.07, respectively, for the normal sample were reported, which indicated a better rolling and tensile performance of the modified compound. The tensile and rupture tests also showed the better mechanical properties of the modified compounds. Finally, the transmission electron microscopy (TEM) images taken from the samples to detect the dispersion of silica demonstrated that the modified mixtures were better than the normal sample.

Zhang et al. [6] synthesized star-shaped copolymers and investigated their mechanical properties. They produced copolymers with arms composed of polybutadiene-polystyrene-butadiene and placed the agents on the ends of the polymer arms using diphenyl hexyl lithium agents. The dispersity of molecular weight distribution of the synthesized copolymers ranged from 1.4 to 1.8 with an average molecular weight of about 280,000 g/mol. They also tried to achieve copolymers with 26% styrene and a functionalization efficiency of more than 50% (66% ultimately). They used DMTA to measure changes in $\tan(\delta)$ values with temperature and used its values as an indicator of assessing the rolling properties and tire slip. It is reported that the sample with a lower rolling resistance showed a better adhesion compared to a similar sample containing carbon black.

Suzuki et al. [25] studied the effect of rubber–filler interaction on stress–strain behavior of styrene-butadiene rubber. The interaction of rubber and filler was controlled by modifying the silica surface using a variety of static coupling agents. Electron spin resonance reflectance and stress–strain test results demonstrated that at a given strain, tensile stress increased with enhancing the interaction between the rubber and filler molecules, and the chain cuts became significant. In this study, two silane bonding agents, namely, TESPT and decyltrimethoxysilane (DC), were utilized to determine

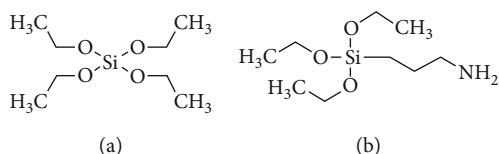


FIGURE 2: The chemical structure of polymer chain functionalization agents: (a) tetraethyl orthosilicate (TEOS); (b) (3-Aminopropyl)triethoxysilane (APTES).

the silica adhesion to the rubber. The results of the TEM images confirmed that the samples with the TESPT coupling agent had a better adhesion to the rubber, and the contact between the rubber and the filler further improved.

Bai et al. [26] investigated the effect of functionalization on the processability and mixing time of the filler with rubber. They examined the mixing time using two different functionalized SBRs and a normal sample. It is shown that the normal sample reached a constant torque later than the two functionalized samples, which implies complete mixing of the silica with the rubber. It is concluded that increasing the interaction of silica with rubber leads to better processability and lower energy consumption during mixing process.

In this study, two types of styrene-butadiene copolymers were synthesized with the addition of silane functional groups to the end of the copolymer chains, and their final properties were compared with those of an ordinary solution synthetic rubber. Also, a mixture using silane coupling agent and a mixture using industrial E-SBR rubber were prepared to compare the properties of the synthesized copolymers with those of the first three mixtures. Totally, five mixtures were subjected to various mechanical, dynamic, and thermal analyses. Various parameters of the functionalized SBR rubber such as torque changes in the internal mixer, bound rubber content, rubber curing, and surface morphology were analyzed. Furthermore, different tests, including hardness test (Shore A), abrasion test, dynamic mechanical thermal analysis, tensile, and rupture test, were also conducted to characterize the synthesized rubbers. Also, it should be noted that we attempted to use an amount of this material equal to that of TEOS and APTES in other mixtures in terms of molarity so that the results are comparable.

2. Experimental

The materials used in this study, as well as the polymerization reactor apparatus, were thoroughly described in our previous work. Similarly, the procedure for the synthesis of the raw rubber and the copolymerization method were explained in detail therein [27].

The used materials are the following: styrene monomer (an extrapure grade), n-hexane (Daejung Company), THF, TEOS, APTES (analytical grade-Sigma Aldrich Company), n-butyllithium 15% in n-hexane (analytical grade-Merck Company), precipitated silica (Evonik Degussa, BET surface area 175 m²) as the reinforcing filler, zinc oxide (ZnO), stearic acid (CH₃(CH₂)₁₆COOH), treated distillate aromatic extracted oil (TDAE), tetramethyl thiuram disulfide (TMTD) and mercaptobenzothiazole (MBT) accelerators, sulfur, and

antioxidant (styrenated phenol) as additives in the curing package, and Nitrogen gas (99.999%). The polymerization reactor apparatus consisting of a 200 ml stainless steel stirred tank with 2 charging and discharging valves (ball and needle valves) was also fabricated in the laboratory and used for this study.

2.1. Compounding and Vulcanization. Compounding stage was performed right after the synthesis. All the compounds were prepared using a recipe described in ref [27] according to the ingredients and their amounts presented in Table 1. Stearic acid, silica, TDAE oil, and antioxidant were all mixed with rubber in a Brabender W50 internal mixer with a Banbury rotor. Then, according to the information given in Table 2, the compounding was done. The final mixing time was started at 50°C and kept for 12 min in order to reach a temperature in the range of 120–140°C. This range of the final temperature is selected in order to guarantee reasonable rate and efficiency of condensation reactions between silica and ethoxy groups.

The heat produced during the mixing can cause cross-linking. To prevent it, the other components, that is, the curing package including sulfur and accelerators, were mixed in a lab open two-roll mill at a roll temperature of 50°C. The two-roll mill has a front roller with 15 rpm and a rear roller with 20 rpm both with the dimeters of 10 cm. In addition, zinc oxide which is reported as a superb activator in sulfur-curing systems was added in the two-roll mill stage [23]. The curing of the compounds was carried out using different specimen molds and under the hot press. The curing conditions were 70 bar and 150°C. The optimum curing time was estimated using a moving die rheometer (MDR).

All the prepared compounds had the same composition, as listed in Table 1; however, one of the compounds was prepared using TESPT silane coupling agent (Si69) in order to investigate the effect of the addition of the silane coupling agent to the polymer chain. To make the results comparable, 0.12 g (0.000233 mol) of the Si69 was added to the compound so that each chain contains one silane coupling agent. Totally, five compounds were prepared and studied in this work where the only difference between them was the type of the utilized copolymer. Table 3 demonstrates how the prepared compounds are named.

2.2. Characterizations

2.2.1. Raw Rubber Characterization. The structural, chemical, mechanical, and thermal properties of the samples were characterized. The Fourier transform infrared (FTIR) demonstrated useful information about the structural properties

TABLE 1: The compounding recipe.

Compound ingredient	Amount (phr)
SSBR	100
Silica	40
TDAE oil	4
ZnO	3
Stearic acid	2.5
TMTD	1.5
MBT	0.5
Sulfur	1.7
Antioxidant	3

TABLE 2: The compounding procedure.

Rotor speed (rpm)	110
Initial temperature (°C)	50
	Time (sec)
Addition of rubber	0
Addition half of silica + stearic acid	90
Addition half of silica + oil + antioxidant	150
Removing material at 150°C	700

TABLE 3: The naming format of the prepared samples.

Sample	Utilized copolymer
E-SBR	Commercial emulsion SBR
S-SBR	Synthetic solution SBR
Si69-SSBR	S-SBR functionalized with Si69
T-SSBR	S-SBR functionalized with TEOS
A-SSBR	S-SBR functionalized with APTES

specifically related to the detection of molecular groups and hence the probable structure of the compounds. In this work, FTIR was employed to ensure the synthesis correctness and confirm the presence of the bonds between the copolymer and the silane coupling agents. The average molecular weight and the polymer dispersity were measured using gel permeation chromatography (GPC). There are some other properties which were all confirmed by hydrogen nuclear magnetic resonance (H-NMR) such as the styrene content and the end functionalization correctness and efficiency. The detailed procedure for the abovementioned analyses is completely explained in our previous publication [27].

2.2.2. Investigation of Torque Changes in Internal Mixer. To investigate the trend of the compound behavior during mixing, the torque changes of the internal mixer versus time were measured. There are some parameters that can be obtained from this diagram: The initial and final torque which show the amount of bonding between the filler and the copolymer and the black incorporation time (BIT) which is a measure of the compatibility of the copolymer with the filler [28].

2.2.3. Bound Rubber Content. The bonding of the filler to the rubber and the interaction between the polymer chains and the filler particles occur either physically or chemically and are not easily separated by the polymer solvent. In filled compounds, the amount of filler bonding to the rubber affects the curing properties and the physical properties of the compound.

In this test, to determine the binding of fillers to rubber, 0.475 g of unfilled compound was dissolved in 10 ml of toluene for six days and then in n-hexane for one day at room temperature in order to extract the copolymer chains having no binding to filler. During this time, the toluene solvent was changed once a day.

The samples were dried for two days at room temperature and then for three hours in a vacuum oven at 50°C. The percentage of binding to the rubber can be calculated by measuring the initial and final weight of the sample as expressed in Equation (1) [29]:

$$R_b(\%) = \frac{100 \times \{W_{fg} - W_t [m_f / (m_f + m_r)]\}}{W_t [m_f / m_f + m_r]}, \quad (1)$$

where R_b is the percentage of binding to the rubber, W_{fg} stands for the final weight of the sample after drying, W_t represents the initial weight of the sample, m_r indicates the rubber percentage in the compound, and m_f denotes the filler percentage in the compound.

2.2.4. Rubber Curing. Curing parameters such as scorch time (ts5), optimum curing time (tc90), and the maximum and minimum difference of torque (MH-ML) were measured by a Gotech M-2000 N moving die rheometer (GOTECH Testing Machines Inc., Taiwan). The rubber compounds were tested at a pressure of 4.6 bar, a temperature of 150°C, and an oscillating angle of $\pm 1^\circ$ arc. Six grams of the compounded rubber with all the ingredients was put in the device, and the testing time was chosen 35 min in order to observe the rubber behavior in an adequate time.

2.2.5. Investigation of Surface Morphology with Field Emission Scanning Electron Microscopy. The surface morphology of the cured compound was examined by field emission scanning electron microscopy (FE-SEM). Scanning electron microscopy imaging is a method by which the amount of accumulated silica particles and their homogeneity can be qualitatively observed. For this purpose, first, the temperature of the cured samples was significantly reduced using liquid nitrogen. Then, the brittle rubber was broken, and the cross section of the fracture was imaged. TESCAN FE-SEM microscope with the voltage of 15 kV was used for this analysis.

2.2.6. Hardness Test (Shore A). The hardness of the rubber is a measure of how rigid it is against a constant pressure that it usually has to withstand during the application. It rises with increasing the filler content and decreases with better material dispersion [30]. The hardness test of the cured samples was done using Frank (Germany) apparatus at 25°C according to standard ASTM D2240. The most conventional

method for evaluating the hardness of rubber is the Shore A test. In this method, the amount of depression in the sample is measured using a needle with an incomplete cone tip and a standard spring. In this work, the test was performed three times at different intervals for each sample to report its mean value as a result [31].

2.2.7. Abrasion Test. DIN abrasion test was employed to measure the wear resistance of the cured samples. To this end, the cured cylindrical rubber samples with a diameter of 15 mm and a height of 6 mm were prepared using compression molding under hot press at a temperature of 150°C. The samples were then placed inside the abrasion test apparatus, Frank (Germany). The test was stopped after a distance of 40 meters from each sample. The changes in the length and mass of the samples were also measured at the beginning and at the end of the test. The S-SBR sample was considered as the reference sample for this test, and the abrasion resistance index (ARI) for the other samples, I_{AR} , was calculated by Equation (2).

$$I_{AR} = \frac{\Delta m_t \cdot \rho_r}{\Delta m_r \cdot \rho_t} \times 100, \quad (2)$$

where Δm_r and ρ_r are the mass changes and density of the reference sample, respectively. Similarly, Δm_t and ρ_t are the mass changes and density of the test sample, respectively.

2.2.8. Dynamic Mechanical Thermal Analysis. DMTA, as one of the thermal analyses for identifying the polymer behavior, was employed to determine glass transition temperature of the compounds. It involves applying a sinusoidal strain to a sample and measuring the mechanical response as a function of the oscillation frequency and temperature; it can be used to measure the modulus and damping ($\tan(\delta)$) in order to specify the rheological and thermal properties of a wide range of compounds. In this analysis, the sample was placed in the device with an appropriate frequency, amplitude, and temperature range set as the input data. Then, the device applied sinusoidal stress to the sample in a known temperature range, and the mechanical response of the material was measured in a controlled temperature environment.

When the stress (σ) is applied to the material, the resulting displacement or rather strain (γ) is measured. For a perfectly elastic solid, the resulting strain and the stress will be perfectly in phase. For a purely viscous fluid, there is a 90-degree phase lag of the strain with respect to the stress. Viscoelastic polymers have the characteristics in between, where some phase lag occurs during DMA tests. When the stress is applied, the strain lags behind, Equation (3) holds for the total stress (4):

$$\sigma = \sigma_0 \sin(\omega t) \cos(\delta) + \sigma_0 \cos(\omega t) \sin(\delta), \quad (3)$$

where ω is the frequency of the strain oscillation, t represents time, and δ indicates the phase lag between the stress and the strain. The storage modulus (G'), which measures

the stored energy and represents the elastic portion, and the loss modulus (G''), which measures the energy dissipated as heat and represents the viscous portion, are defined as Equations (4) and (5), respectively:

$$G' = \frac{\sigma_0}{\gamma_0} \cos(\delta), \quad (4)$$

$$G'' = \frac{\sigma_0}{\gamma_0} \sin(\delta). \quad (5)$$

The ratio of the storage modulus to the loss modulus, i.e., $\tan(\delta)$, is a measure of the system damping (Equation (6)).

$$\tan \delta = \frac{G''}{G'} \quad (6)$$

In this study, the samples were all prepared in the form of rectangular cubes with a length of 25 mm, a width of 4 mm, and a thickness of 2 mm. A temperature range of -100 to 100°C, a frequency of 10 Hz, a strain amplitude of 0.1%, and a temperature ramp of 2°C/min were considered for this analysis. Also, in order to plot the G' change versus strain, the G' values were measured at 60°C at a frequency of 10 Hz at strain values of 0.1%, 1%, 10%, and 100%.

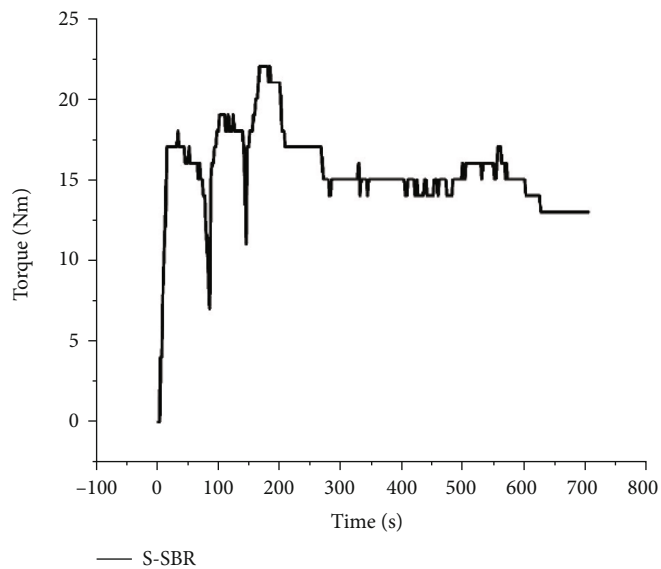
2.2.9. Tensile and Rupture Test. In order to obtain the tensile resistance and the rupture of the cured compounds, tensile and rupture tests were conducted using dumbbell-shaped samples by universal electronic machine, GoTech AL-3000 according to standards ASTM D412 and ASTM D624, respectively. The samples were stretched at 25°C at a rate of 500 mm/min.

3. Results and Discussion

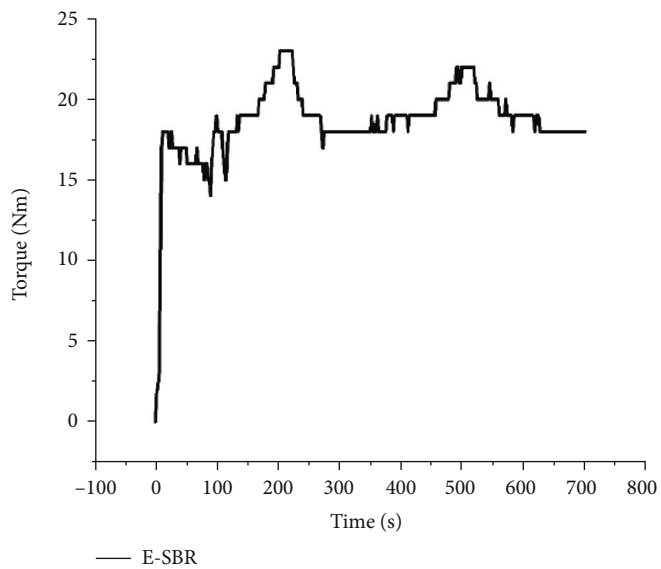
3.1. Fourier Transform Infrared Spectrometry, Gel Permeation Chromatography, and Nuclear Magnetic Resonance. The FTIR spectra of the synthesized samples, namely, A-SBBR, T-SBBR, and S-SBR, were recorded from thin films of them. The S-SBR, T-SBBR, and A-SBBR samples were separately characterized. A comprehensive discussion about these results, as well as the gel permeation chromatography and hydrogen nuclear magnetic resonance results, was made in our previous publication.

3.2. Investigation of Torque Changes in Internal Mixer. During the mixing process in the internal mixer, the torque of the device was observed as a criterion for observing the behavior of the viscous rubber. These data are plotted for each sample in Figure 3.

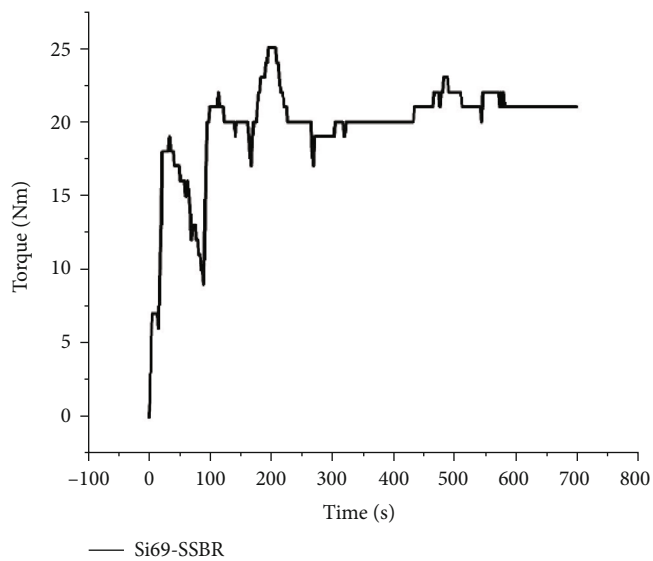
In a typical diagram of the filled rubber mixtures, three main regimes are observed. In the first regime, by adding a polymer into the machine and breaking it into small pieces inside the machine, the torque suddenly increases. This is followed by the homogeneity of the material inside the mixer and a slight increase in temperature which leads to a gradual reduction in the amount of torque. The second regime, when the filler is added to the copolymer, is characterized by a



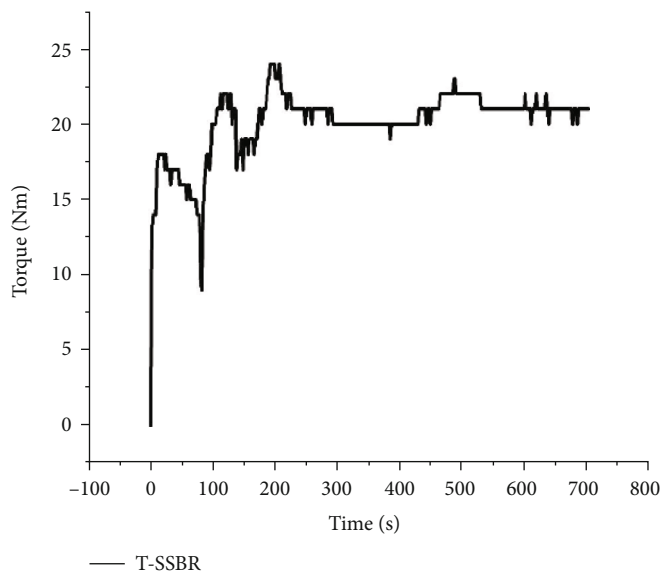
(a)



(b)



(c)



(d)

FIGURE 3: Continued.

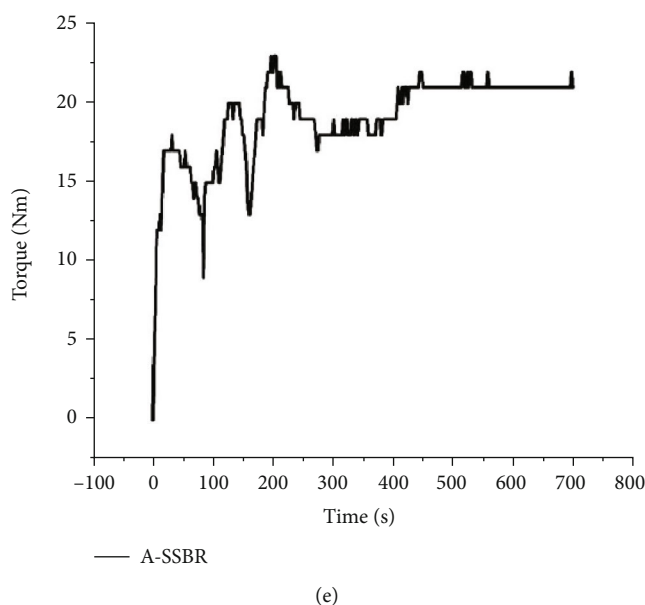


FIGURE 3: Graphs of torque changes over time for different mixtures: (a) S-SBR, (b) E-SBR, (c) Si69-SBR, (d) T-SBR, and (e) A-SSBR.

sudden increase in the torque. This sudden increase is due to the rise in the volume of the mixture inside the chamber; the pressure applied to the inlet chamber due to the lever; and the tightness, compression, and rupture of the mixture in the space between the mixer wall and the blades. At the end of this regime, by adding the filler, increasing the chamber temperature, and placing the filler particles completely inside the copolymer, the rotor rotates again easier and the amount of the torque is reduced.

In the third regime, the filler particles and other rubber additives have a better and more effective penetration into the rubber and form a homogeneous mixture. Shear and tensile deformation of the rubber inside the chamber puts new layers and new surfaces of rubber in front of the fillers, and eventually the majority of the copolymer surfaces come in contact with the filler. These new surfaces, while absorbing filler and other additives, adhere to other rubber surfaces and form larger masses of the mixture, which slightly increases the torque of the machine. The peak point of this area is the BIT or filler mixing time. Then, as the temperature rises and the filler particles completely disperse into the rubber and reach the final level of homogeneity, the rotor torque declines again and reaches a constant limit.

In samples A-SSBR, T-SSBR, and Si69-SBR, due to the fact that ethoxy branches bond with silica at a temperature higher than 140°C, which increases the strength of the compound and the torque, the third regime was slightly different. In these samples, the torque did not decrease after the BIT peak and remained almost constant. In other words, the peak related to the increase in torque due to silane bonding with the silica surface neutralized the decrease in torque caused by the mixture temperature increase.

In Figure 3, the three regimes are clearly visible. Initially, by adding the rubber to the chamber, the torque began to be recorded. After reaching a certain limit, its value was gradually reduced. In the first and second minutes, when the silica

was added to the rubber, the two regimes with peaks were observed at a time of about 100 and 200 seconds, which was the same peak introduced in the second regime. Also, at a time of 450 to 550 seconds, the weak peak of the third BIT regime was evident.

The initial torque of each sample can be considered as a measure of its thickness. For this purpose, the local minimum of the torque curve just before the silica addition point was observed as a criterion for all the samples. According to the diagrams, this value for the industrial E-SBR sample due to its high amount of styrene was significantly higher compared to the synthetic copolymers. There are some reasons such as the apparatus operation, filling percentage, and the speed or temperature of the addition of the silica which make this quantity very inaccurate and can change the amount of the torque. For this reason, the saturated copolymers with close values of the torque were not compared. The difference between the initial and final torques of the compounds can be used as a measure of a high amount of bonding between silica and rubber, which resulted in the increased viscosity of the mixture [26]. Figure 4 shows the difference between the initial and final torques of the mixtures.

The increase in the torque or viscosity of the mixture in the samples containing silane modifications was clearly greater, which indicates a better filler-copolymer interaction and an enhanced dispersion of silica between the rubber and its bond. The obtained BIT values for the different mixtures are given in Table 4.

As mentioned, the BIT is a measure of the ease of the filler mixing in rubber [26]. It is shown that silane-modified rubbers were more successful in distributing silica among themselves, which is due to the attraction between the agents on the copolymer chains and the coupling agent on the silica surface. Meanwhile, A-SSBR was more easily combined with the filler using the hydrogen bonding of its

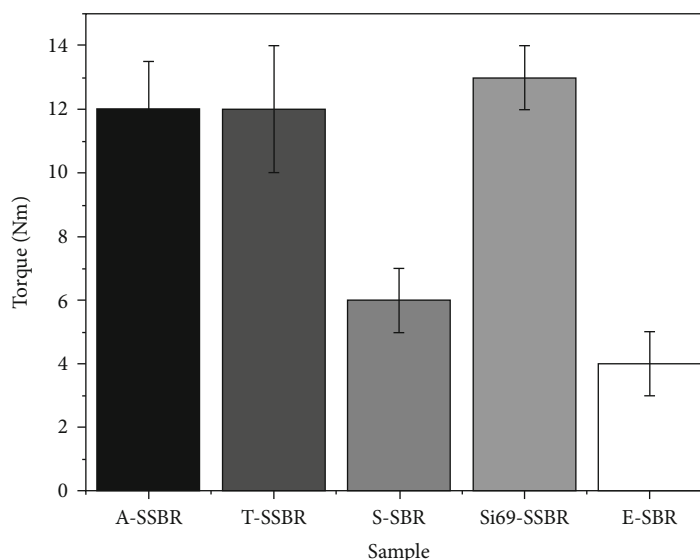


FIGURE 4: The difference between the initial and final torques of the mixtures.

TABLE 4: Filler mixing time (BIT) for the different mixtures.

Sample	BIT (s)
S-SBR	554
E-SBR	516
Si69-SSBR	490
T-SSBR	488
A-SSBR	449
S-SBR	554

TABLE 5: The calculated bound rubber contents of the samples.

Sample name	Secondary weight (g)	Bound rubber content (%)
S-SBR	0.157	6.9
T-SSBR	0.279	42.1
A-SSBR	0.321	55.5
E-SBR	0.167	10.2
Si69-SSBR	0.298	48.2

TABLE 6: Curing specifications of the mixtures.

Curing specification	S-SBR	T-SBR	A-SSBR	E-SBR	Si69-SSBR
Ts5 (m)	2.39	2.34	2.33	2.49	1.08
Tc90 (m)	7.39	6.21	6.09	6.58	3.53
MH (Nm)	3.17	4.2	6.02	3.85	4.75
ML (Nm)	1.58	2.16	3.21	1.82	2.56
MH-ML (Nm)	1.59	2.04	2.81	2.03	2.19

amino hydrogens than the two other copolymers that required a chemical reaction for bonding to the silica.

3.3. Bound Rubber Content. The bound rubber content was calculated by Equation (1) by considering the values of 0.25, 0.64, and 0.475 for the rubber percentage, the filler per-

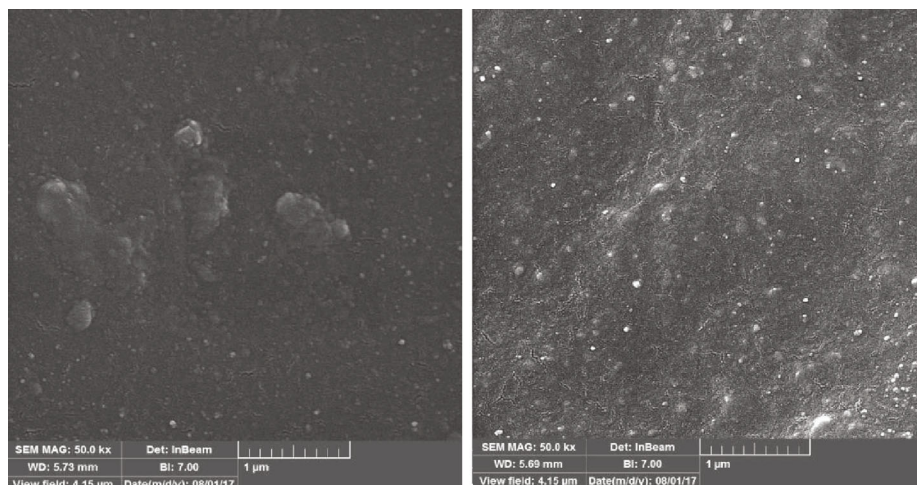
centage, and the initial weight of each sample, respectively. Table 5 presents the bound rubber content of each sample.

The bound rubber content is affected by the filler-polymer interaction. In Table 5, samples A-Si69-SSBR, SSBR, and T-SSBR showed high amounts of bonding to the rubber, indicating greater chemical bonds between the copolymer chains and the silica particles. This performance of the compounds was the result of the end functionalization of the chains in the two functionalized samples and the use of silane coupling agent in sample Si69-SSBR. The lower bound rubber content in sample T-SSBR compared to the two other modified samples, especially the sample with silane coupling, can be explained by the lower efficiency of this copolymer compared to the others. Sample A-SSBR also showed the best performance due to the utilizing of both types of ethoxy and amine branches.

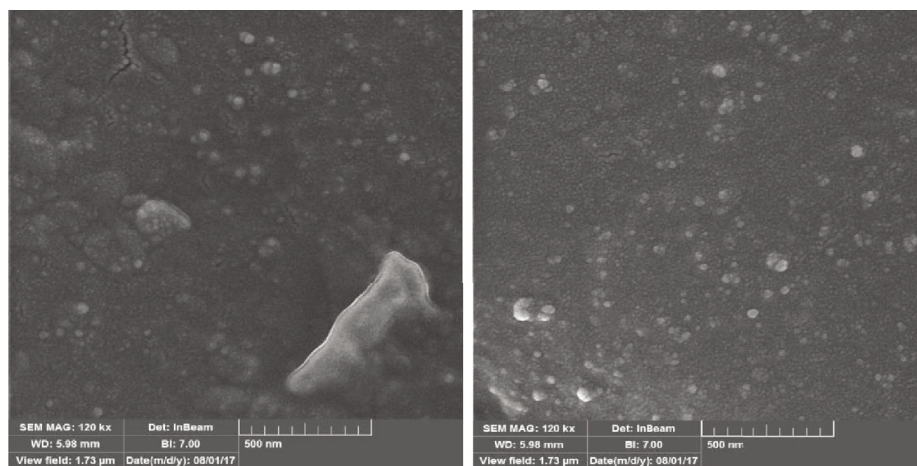
3.4. Rubber Curing. The required parameters obtained from the torque diagrams of the mixtures are listed in Table 6.

Since the rubber curing operation is a heat treatment, the amount of curing of the rubber largely depends on its thermal conductivity. The thermal resistance of styrene-butadiene rubber is between 0.2 and 0.25 W/m-K, and this quantity for silica is about 4.1 W/m-K. Therefore, with the addition of the silica to the rubber, an increase in the thermal conductivity of the compound was observed. At the same time, as the distribution of acetyl acetate in the rubber increased, this increase in the thermal flux occurred better. The result is a reduction in scorching and curing times, which occurs due to the faster conduction of heat to the whole mixture [32].

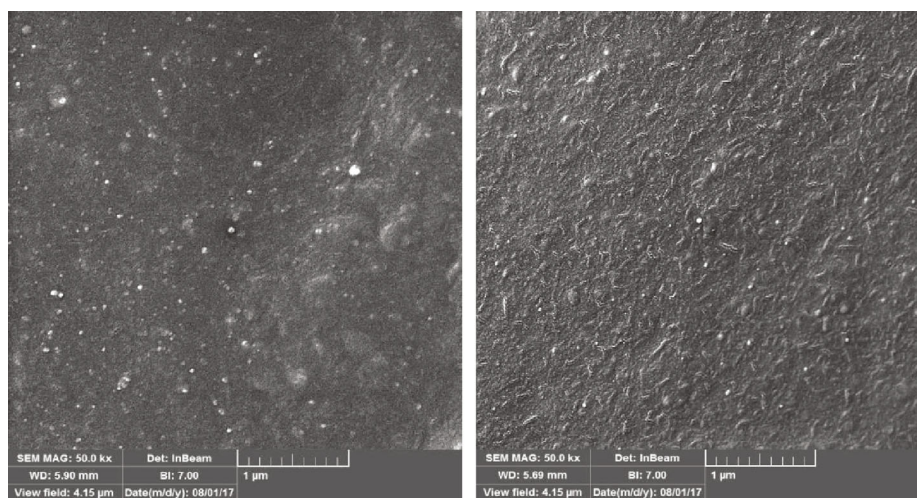
According to Table 6, the minimum curing and scorching times were related to the modified mixtures, which proves that the use of copolymers with functionalized chains helped to disperse the silica in the rubber. This proper dispersion resulted in a better thermal conductivity. The lowest value was for compound Si69-SSBR, which was significantly lower than that of the other compounds. This can be



(a)



(b)



(c)

FIGURE 5: Continued.

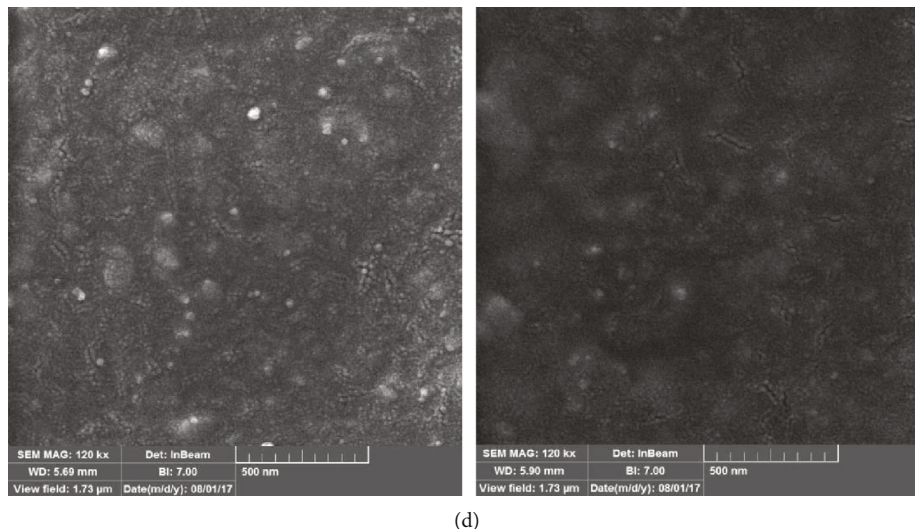


FIGURE 5: SEM images of: (a) S-SBR, (b) Si69-SSBR, (c) T-SBR, and (d) A-SSBR at two magnifications of $\times 50,000$ and $\times 120,000$.

explained due to the additional amount of sulfur associated with this mixture, as well as the better diffusion of silica due to the use of coupling agent, because the added coupling agent (TESPT) itself contained four sulfur atoms, which increased the amount of the crosslinks.

The minimum of the torque curve (ML) can be directly related to the viscosity of the mixture. The order of these mixtures in reducing the viscosity was similar to the order of the final torque of the mixtures created by the internal mixer; these two tests can confirm each other very well.

The minimum (ML) and maximum (MH) torques are affected by the filler network and the connection to the rubber. The difference between them in the curing rheometer torque curve is a measure of the amount of amplification, the physical effects of the filler in the matrix, and the amount of curing and the crosslinks created in the matrix. Due to the uniformity of the curing package of all the mixtures, the amount of MH–ML in this test mainly indicates the effects of the filler on the rubber reinforcement.

The enhanced dispersion of silica in the mixtures with functionalized copolymer increased the torque, which was higher in sample A-SSBR compared to the others. This indicated a better silica diffusion in the rubber and the end agent of this copolymer. Also, the increase in sulfur crosslinks due to the sulfur presence in the coupling agent made sample Si69-SSBR second in terms of torque and higher than the modified T-SSBR copolymer.

3.5. Investigation of Surface Morphology with Field Emission Scanning Electron Microscopy. Imaging of the cured mixture inner surfaces clarifies reliable information about the silica placement or their possible accumulations inside the mixture. These images were taken at two magnifications of $\times 50,000$ and $\times 120,000$. Samples T-SSBR, Si69-SSBR, S-SBR, and A-SSBR were selected for imaging (Figure 5). The bright points represent silica aggregation, and the larger points indicate a higher density of silica.

It is found out that the size of these particles in sample S-SBR was larger than that of the other samples, which was expected due to the lack of modifications in this mixture. It is shown that silica had the tendency to form its round aggregates and was unwilling to interact with a nonpolar polymer completely. Samples Si69-SSBR and T-SSBR demonstrated almost identical results due to their almost identical silica bonding through the ethoxy branches of the modifiers. Moreover, the silica aggregate sizes of them were much smaller. The A-SSBR compound contained smaller aggregates of silica due to its higher polarity than the other two modified compounds.

Figure 6 illustrates the silica mapping in the mixtures using EDS mapping technique. For this purpose, Si element, which was supplied only in the mixture silica surface, was detected at a magnification of about $\times 150,000$. In these images, Si can be seen as the red dots, and the density of the dots represents the Si density on the surface. Furthermore, the Si dispersion in the functionalized copolymers was better than that in the unmodified copolymers, and sample A-SSBR had an enhanced silica dispersion because of its higher polarity and larger number of physical and chemical bonds.

3.6. Hardness Test (Shore A). At the filler loads of higher than 20%, the distance between the silica aggregates is such small that it can induce strong interactions between them and create another network so called filler–filler network. These networks increase the hardness of the rubber. In the case of using silica as the filler, the filler hardness percentage is about 50%, which makes it harder than that of carbon black (30%) [33]. Also, the formation of these filler networks reduces the mobility and deformation of the copolymer macromolecules and adds to the hardness of the compound [6, 30]. The hardness test (Shore A) results of the samples are presented in Figure 7.

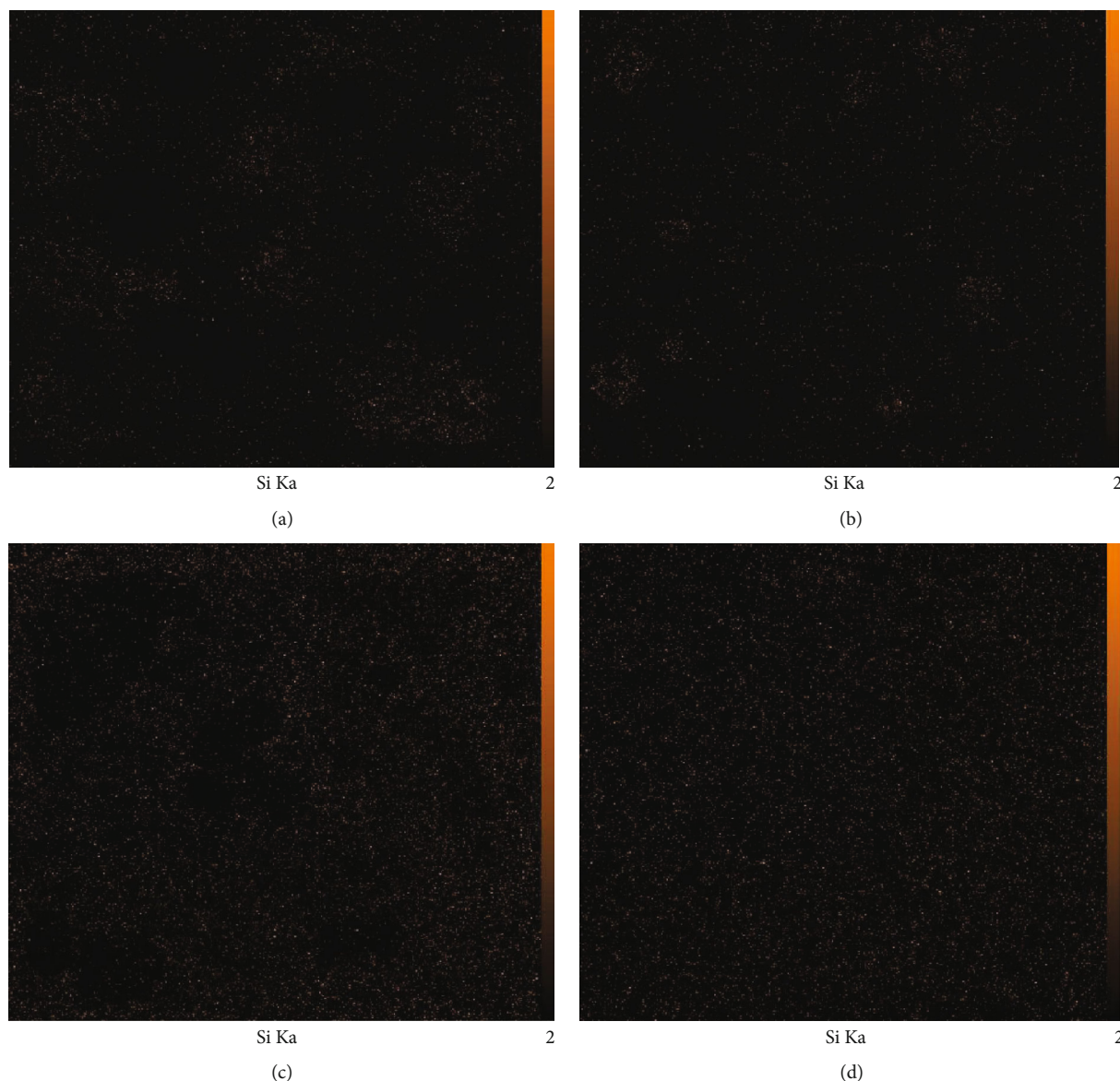


FIGURE 6: Silica mapping in (a) S-SSBR, (b) Si69-SSBR, (c) T-SSBR, and (d) A-SSBR.

It is clear that the last three compounds showed a higher hardness value owing to the modifications to the polymer chain and the addition of a coupling agent than the two other conventional SBRs, which can be attributed to the reduction in the networks between the fillers. Among the functionalized rubbers, sample A-SSBR performed better, as it was expected, mainly because of using two types of silica bonds provided by the addition of the amino branch. Also, the mixture with the silane coupling agent demonstrated a result similar to that of the functionalized sample.

3.7. Abrasion Test. The results of the abrasion test were calculated using Equation (2) considering a density of 1.22 g/m^3 for the compounds. Figure 8 presents the abrasion test results of the compounds while sample S-SBR was considered as the reference.

It is stated that the abrasion resistance in the filled mixtures improves as the filler dispersion improves [13]. Therefore, it was expected that the mixtures with an enhanced silica dispersion, resulting from the use of silane coupling agents and the introduction of end agents at the end of the copolymer chains, show a better abrasion resistance. Among the modified copolymers, compound A-SSBR had the best performance in the abrasion test. This can be due to the presence of strong bonds between the filler and the end of the copolymer chains, resulted from A-SSBR strong chemical and physical couplings using its autocyclic and amine branches. The other two samples had almost the same results as those of the other tests.

Also, about the two unmodified mixtures, it is found out that the lower glass transition temperature of sample S-SBR made this copolymer superior in the abrasion properties

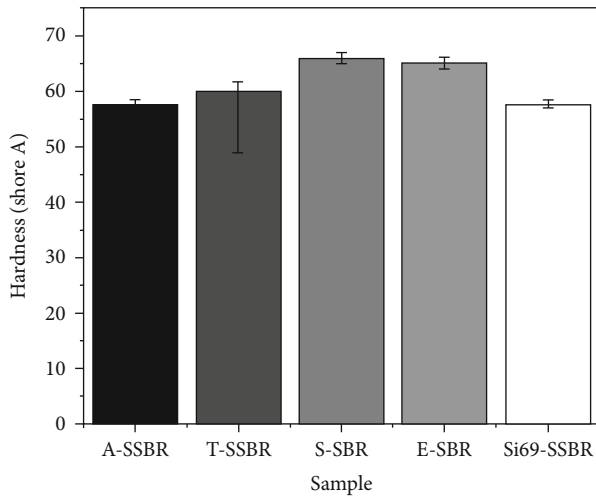


FIGURE 7: The hardness test (Shore A) results of the samples.

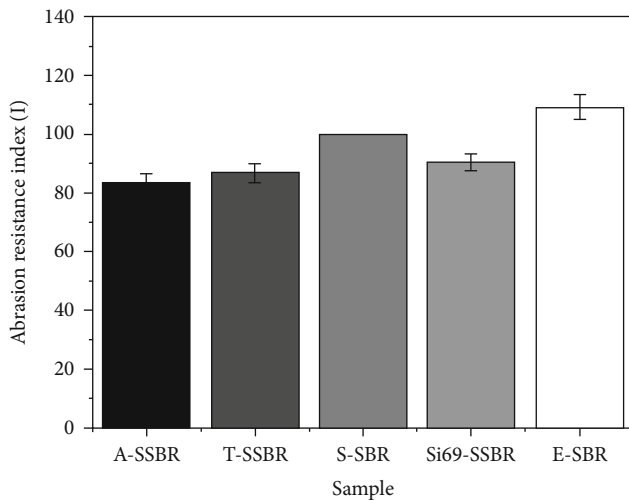


FIGURE 8: The abrasion test results of the samples.

compared to E-SBR. It is confirmed that the copolymers with a lower glass transition temperature generally express better abrasion and rolling properties [34].

3.8. Dynamic Mechanical Thermal Analysis. Figure 9 delineates the DMTA results of the studied copolymers in terms of analyzing the $\tan(\delta)$ diagram at a temperature of 0 and 60°C; $\tan(\delta)$ values in the two regions of -20 to 0°C and 50 to 80°C represent the quality of the mixture in terms of the two characteristics of rolling resistance and wet grip, respectively. Thus, higher values of $\tan(\delta)$ at 0°C indicate a better wet grip, while lower values of $\tan(\delta)$ at 60°C denote lower rolling resistance (better fuel efficiency). At a temperature of 0°C, the mixture containing E-SBR copolymer had the highest value of $\tan(\delta)$. However, its $\tan(\delta)$ value at 60°C was higher than the that of the others. Compounds T-SSBR, Si69-SSBR, and -A-SSBR, which had a silane modifier, were able to improve the values of $\tan(\delta)$ toward more favorable values at a temperature of 0 and 60°C. Although there was a slight regression in the wet grip level of the com-

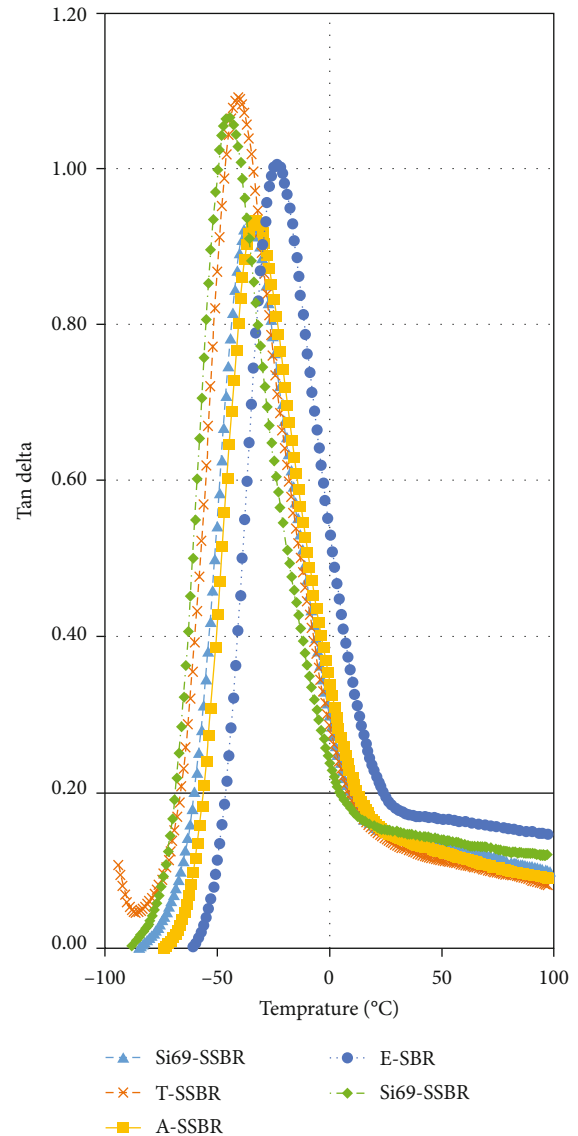


FIGURE 9: The variation in $\tan(\delta)$ with the temperature for the cured samples.

TABLE 7: The glass transition temperature of the mixtures.

	S-SBR	T-SSBR	A-SSBR	E-SBR	Si69-SSBR
Glass transition temperature (°C)	-43	-40	-34	-21	-36

pounds, with the improvement to the silica dispersion in the copolymer and the reduction of filler aggregates, the $\tan(\delta)$, or rather the stress loss (G''), of the compounds decreased. Therefore, it resulted in a reduction of fuel consumption. It is also worth mentioning that the amount of regression is less effective compared to the improvement in the rolling resistance of the compound.

Furthermore, the value of the glass transition temperature of the mixtures, which is equal to the temperature corresponding to the peak of the $\tan(\delta)$ diagram, can be

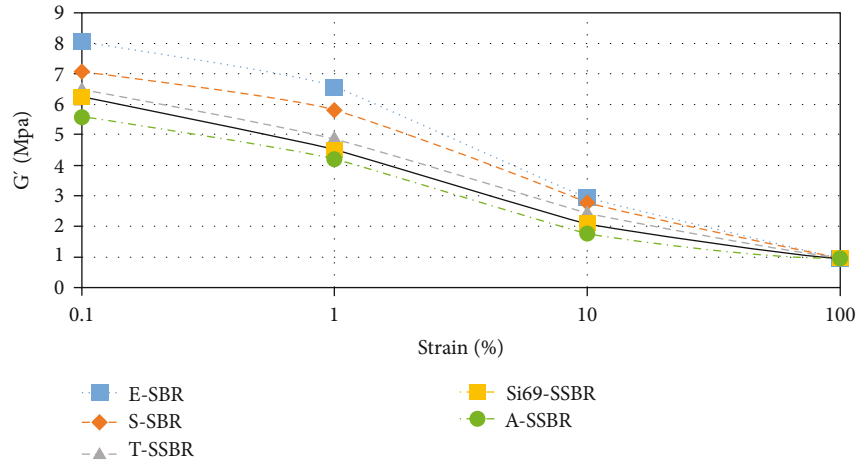


FIGURE 10: The variation in G' with strain.

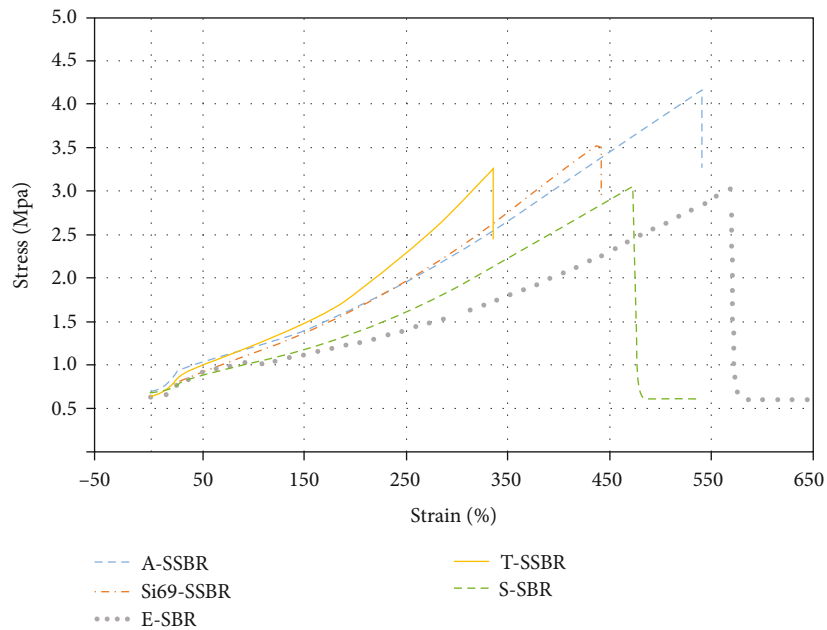


FIGURE 11: The stress–strain diagrams of the tensile test for the cured mixtures.

TABLE 8: The mechanical properties of the cured mixtures from the tensile and rupture tests.

Mechanical properties	Sample name				
	T-SSBR	Si69-SSBR	A-SSBR	E-SBR	S-SSBR
Modulus at 100% elongation (kPa)	1.218 ± 0.05	1.141 ± 0.035	1.198 ± 0.06	1.017 ± 0.021	1.019 ± 0.046
Tensile strength (MPa)	3.260 ± 0.166	3.568 ± 0.147	4.150 ± 0.157	3.028 ± 0.091	3.066 ± 0.125
Elongation at break point (%)	335 ± 10	440 ± 23	539 ± 14	569 ± 24	473 ± 22
Tear strength (kPa)	4015 ± 152	3813 ± 122	4764 ± 214	3064 ± 125	2967 ± 107

obtained from Figure 9. Table 7 lists the corresponding values of each sample.

An increase in T_g of the modified compounds can be related to the changes in the movement rate and behavioral constraints of the copolymer chains attached to the filler. Normally, the similar T_g of the three synthetic copolymers

of this study was expected due to their almost identical molecular mass and microstructure. It is clear that the highest increase in T_g was observed in sample A-SSBR, which can be related to the strengthening of the bonds between the filler and the polymer. The same properties can be mentioned for the two polymers with the other silane

modifications. Hence, it can be concluded that compound S-SBR had the most unfavorable value of $\tan(\delta)$ at 0 and 60°C due to the T_g value.

It is well known that the copolymers with a high T_g and styrene content are typically known for their better wet grip properties. Nonetheless, copolymers with a low T_g are known for better wear and rolling properties, which can also be confirmed for compound E-SBR in comparison to the other samples studied in this work [34, 35].

In order to investigate the Payne effect, the DMTA was performed at a temperature of 60°C, a frequency of 10 Hz, and strain of 0.1%, 1%, 10%, and 100%. As mentioned earlier, the rate of changes in G' by varying the amount of strain indicates the Payne effect. Therefore, lower values are more desirable, which leads to the reduction of the filler aggregates and the decline in the networks formed between fillers. Figure 10 plots the changes in G' versus the strain.

It is shown that the variation of G' in a strain range of 0.1% to 100% of samples Si69-SSBR, T-SSBR, and A-SSBR is less than that of the two mixtures with unmodified copolymers, which indicates the enhanced dispersion of the filler in the copolymer as a result of bonding between silane and filler agents. Among the samples containing silane agents, sample A-SSBR exhibited better and more bonds with the silica surface, which was confirmed by the lower $\Delta G'$ value. This was due to having both amine and ethoxy groups. Samples T-SSBR and Si69-SSBR also showed almost similar results due to the similar bonding between the filler and the silane agents.

3.9. Tensile and Rupture Test. It is well known that the mechanical properties of the cured mixtures are affected by the size of the silica aggregates as well as the filler–rubber interaction [36, 37]. Polmanteer et al. mentioned that the properties such as tear strength and tensile strength are improved with an enhanced silica dispersion, specifically in the case of sulfur-cured rubbers. They also showed that the filler dispersion, the filler–rubber interaction, and the resistance to external force can be enhanced, and the rupture propagation is longer [38].

The tensile and rupture test results are presented in Figure 11 and Table 8, respectively. The results demonstrate that the modified compounds, the enhanced silica dispersion of which was previously confirmed, also offered better mechanical properties. The best properties belonged to sample A-SSBR. Tensile strength, tear, and modulus of this sample had a better average than those of the other samples. The other improved compounds, namely, T-SSBR and Si69-SSBR, also exhibited better results than the samples with weaker dispersion. Sample A-SSBR, as previously stated, had better adsorption and diffusion of silica due to the higher polarity of the functional groups.

The elongation of sample E-SBR was larger than that of the other compounds, which can be explained by the direct relationship between the molecular weight and elongation. Therefore, the higher molecular weight of the industrial sample, i.e., E-SBR, led to a higher elongation. Further, the elongation of the compounds can be different due to the

changes in the microstructure and especially the styrene content; thus, it appears that the lower styrene content of sample A-SSBR compared to that of the other samples was effective in its elongation.

4. Conclusions

Solution polymerization is known as an alternative method for the synthesis of styrene-butadiene copolymers. The advantages of this method, along with the superior properties of the produced copolymer, can possibly reduce the production costs compared to the previous methods, which has helped this method receive significant attention. In addition, the possibility of using the living copolymer chains to add desirable properties to the product is another reason for the interest in this issue. The difficulty of dispersing silica in nonpolar compounds and the influence of silica dispersion on the final properties of the rubber product were the main motivations for this research.

In this study, after synthesizing styrene-butadiene copolymer with a specific and controlled microstructure and macrostructure, medium-vinyl copolymers with a styrene content of about 20% were obtained as targeted initially. The reactions were also completed at a high rate, and by using chain random factors, in addition to increasing the polymerization rate, random copolymers were obtained which are suitable for the desired tire applications.

It was predicted that despite the polar groups on the silica surface and the nonpolarity of the hydrocarbon chains, the interaction and distribution of silica in the rubber is improved as the polarity of the chains increased. Therefore, the introduction of APTES, which has amino chains and can create polar space at the end of the chains, was really of high importance.

The as-synthesized copolymers were analyzed using FTIR, H-NMR, and GPC analyses to characterize the copolymer structure, confirm the presence of TEOS and APTES functional groups in the copolymers, and determine their average molecular weights and molecular weight distributions. A similar compound was then made of industrial emulsion SBR rubber for comparison.

The rheometry test revealed that sample E-SBR had a lower scorching and curing temperature than the other compounds, which was due to the enhanced dispersion of silica in the polar sample. As the filler dispersion enhanced, the heat resistance of the mixture decreased and heat was easily transferred. Also, the difference between the maximum and minimum torques was greater compared to the modified mixtures, which was a measure of the rubber–filler interaction. Sample A-SSBR had the best performance compared to the other modified samples, which revealed the effect of functionalization on the curing quality of the compounds.

The FE-SEM microscopy results also confirmed the enhanced dispersion of silica in the modified samples. The hardness of the cured compounds was also measured using the Shore A test. As expected, a better filler–rubber mixing led to a higher softness of the rubber. Thus, sample A-SSBR was 12% softer than the conventional sample.

The results of the DIN wear test, representing the wear resistance of rubber compounds, indicated that the wear resistance of the modified samples improved compared to the S-SBR compound, the reference sample. In this test, samples A-SSBR and T-SSBR performed 17% and 14% better than the reference sample, respectively.

The DMTA, as one of the most important tests to determine the properties of a cured rubber, was performed to determine parameters $\tan(\delta)$ and G' of the compounds at different temperatures and strains. The sample modified with APTES had a better performance in this area and was able to have a better balance between the rolling resistance and wet surface grip. The other modified compounds also performed better than the S-SBR reference sample. It should be noted that the used industrial E-SBR sample, due to its high styrene content, was not exactly comparable with the other samples. The test also reported the value of G' at different strains. The lowest value was related to modified sample A-SSBR. The other modified samples also performed better than the conventional E-SBR, indicating a positive effect of polymer chain modification on filler dispersion.

According to the tensile and rupture tests, the tensile strength of the modified compounds was much higher than that of the S-SBR reference rubber. All of the improved samples had better performance than the S-SBR sample. Sample A-SSBR performed best with a tensile strength 37% larger than that of the S-SBR. The modified mixtures had almost similar elongations at break point. Only the industrial E-SBR rubber had a somehow close performance to them due to its high molecular weight.

Finally, the results of all the analyses clearly demonstrated that matching the intermolecular forces between the filler and the rubber ultimately led to an enhanced filler dispersion in the matrix, which gave rise to the superior properties of the synthesized and modified samples. The S-SBR copolymer delivered the best overall performance by placing APTES at the end of its chains. The TEOS had less polarity but more covalent chain bonding. It also performed better than the conventional S-SBR sample, and the results confirmed that the performance of this sample was identical to that of the sample with the silane coupling agent.

Data Availability

The experimental data used to support the findings of this study are available from the corresponding author upon request.

Conflicts of Interest

The authors declare that they have no conflicts of interest.

References

- [1] S. Ahmadian-Fard-Fini, D. Ghanbari, O. Amiri, and M. Salavati-Niasari, "Electro-spinning of cellulose acetate nanofibers/Fe/carbon dot as photoluminescence sensor for mercury (II) and lead (II) ions," *Carbohydrate Polymers*, vol. 229, article 115428, 2020.
- [2] D. Vanitha, S. A. Bahadur, N. Nallamuthu, S. Athimoolam, and A. Manikandan, "Electrical impedance studies on sodium ion conducting composite blend polymer electrolyte," *Journal of Inorganic and Organometallic Polymers and Materials*, vol. 27, no. 1, pp. 257–265, 2017.
- [3] S. Saeedi Garakani, M. Khanmohammadi, Z. Atoufi et al., "Fabrication of chitosan/agarose scaffolds containing extracellular matrix for tissue engineering applications," *International Journal of Biological Macromolecules*, vol. 143, pp. 533–545, 2020.
- [4] Z. Atoufi, S. K. Kamrava, S. M. Davachi et al., "Injectable PNI-PAM/hyaluronic acid hydrogels containing multipurpose modified particles for cartilage tissue engineering: synthesis, characterization, drug release and cell culture study," *International Journal of Biological Macromolecules*, vol. 139, pp. 1168–1181, 2019.
- [5] S. Ahmadian-Fard-Fini, D. Ghanbari, and M. Salavati-Niasari, "Photoluminescence carbon dot as a sensor for detecting of *Pseudomonas aeruginosa* bacteria: hydrothermal synthesis of magnetic hollow NiFe_2O_4 -carbon dots nanocomposite material," *Composites. Part B, Engineering*, vol. 161, pp. 564–577, 2019.
- [6] S. Zhang, S. Zhao, X. Zhang, L. Zhang, and Y. Wu, "Preparation, structure, and properties of end-functionalized microarms star-shaped polybutadiene-*sn*-poly(styrene-butadiene) rubber," *Journal of Applied Polymer Science*, vol. 131, no. 6, 2014.
- [7] V. Parameswaran, N. Nallamuthu, P. Devendran, A. Manikandan, and E. R. Nagarajan, "Assimilation of NH_4Br in polyvinyl alcohol/poly(N-vinyl pyrrolidone) polymer blend-based electrolyte and its effect on ionic conductivity," *Journal of Nanoscience and Nanotechnology*, vol. 18, no. 6, pp. 3944–3953, 2018.
- [8] K. Sundaramahalingam, N. Nallamuthu, A. Manikandan, D. Vanitha, and M. Muthuvinayagam, "Studies on sodium nitrate based polyethylene oxide / polyvinyl pyrrolidone polymer blend electrolytes," *Physica B: Condensed Matter*, vol. 547, pp. 55–63, 2018.
- [9] V. Parameswaran, N. Nallamuthu, P. Devendran, E. R. Nagarajan, and A. Manikandan, "Electrical conductivity studies on ammonium bromide incorporated with zwitterionic polymer blend electrolyte for battery application," *Physica B: Condensed Matter*, vol. 515, pp. 89–98, 2017.
- [10] F. Davar, M. Salavati-Niasari, and Z. Fereshteh, "Synthesis and characterization of SnO_2 nanoparticles by thermal decomposition of new inorganic precursor," *Journal of Alloys and Compounds*, vol. 496, no. 1-2, pp. 638–643, 2010.
- [11] C. K. Hong, H. Kim, C. Ryu, C. Nah, Y. Huh, and S. Kaang, "Effects of particle size and structure of carbon blacks on the abrasion of filled elastomer compounds," *Journal of Materials Science*, vol. 42, no. 20, pp. 8391–8399, 2007.
- [12] H. Jeon, Y. Kim, W.-R. Yu, and J. U. Lee, "Exfoliated graphene/thermoplastic elastomer nanocomposites with improved wear properties for 3D printing," *Composites. Part B, Engineering*, vol. 189, article 107912, 2020.
- [13] B. Seo, K. Kim, H. Lee, J. Y. Lee, G. H. Kwag, and W. Kim, "Effect of styrene-butadiene rubber with different macrostructures and functional groups on the dispersion of silica in the compounds," *Macromolecular Research*, vol. 23, no. 5, pp. 466–473, 2015.
- [14] L. A. E. M. Reuvekamp, J. W. ten Brinke, P. J. van Swaij, and J. W. M. Noordermeer, "Effects of time and temperature on the

- reaction of TESPT silane coupling agent during mixing with silica filler and tire rubber," *Rubber Chemistry and Technology*, vol. 75, no. 2, pp. 187–198, 2002.
- [15] C. J. Lin, T. E. Hogan, and W. L. Hergenrother, "On the filler flocculation in silica and carbon black filled rubbers: part II. Filler flocculation and polymer-filler interaction," *Rubber Chemistry and Technology*, vol. 77, no. 1, pp. 90–114, 2004.
- [16] S.-S. Choi and C. E. Son, "Influence of silane coupling agent on bound rubber formation of NR/SBR blend compounds reinforced with carbon black," *Polymer Bulletin*, vol. 73, no. 12, pp. 3453–3464, 2016.
- [17] W. Wu and F. Chen, "Interfacial modification of corn stalk cellulose reinforced used rubber powder composites treated with coupling agent," *Journal of Renewable Materials*, vol. 8, no. 8, pp. 905–913, 2020.
- [18] Q. Tian, Y. Tang, T. Ding, X. Li, and Z. Zhang, "Effect of nano-silica surface-capped by bis[3-(triethoxysilyl)propyl] tetrasulfide on the mechanical properties of styrene-butadiene rubber/butadiene rubber nanocomposites," *Composites Communications*, vol. 10, pp. 190–193, 2018.
- [19] S. Radabutra, P. Khemthong, and S. Saengsuwan, "Effect of silane coupling agent pretreatment on the properties of rice straw particleboard bonded with prevulcanized natural rubber latex," *Journal of Rubber Research*, vol. 24, no. 1, pp. 157–163, 2021.
- [20] E. Padenko, P. Berki, B. Wetzel, and J. Karger-Kocsis, "Mechanical and abrasion wear properties of hydrogenated nitrile butadiene rubber of identical hardness filled with carbon black and silica," *Journal of Reinforced Plastics and Composites*, vol. 35, no. 1, pp. 81–91, 2016.
- [21] H. Dohi and S. Horiuchi, "Locating a silane coupling agent in silica-filled rubber composites by EFTEM," *Langmuir*, vol. 23, no. 24, pp. 12344–12349, 2007.
- [22] X. Liu, S. Zhao, X. Zhang, X. Li, and Y. Bai, "Preparation, structure, and properties of solution-polymerized styrene-butadiene rubber with functionalized end-groups and its silica-filled composites," *Polymer*, vol. 55, no. 8, pp. 1964–1976, 2014.
- [23] S. Maghami, W. K. Dierkes, and J. W. M. Noordermeer, "Functionalized SBRs in silica-reinforced tire tread compounds: evidence for interactions between silica filler and zinc oxide," *Rubber Chemistry and Technology*, vol. 89, no. 4, pp. 559–572, 2016.
- [24] V. M. Il'in and A. K. Rezova, "Styrene butadiene rubber: production worldwide," *International Polymer Science and Technology*, vol. 42, no. 10, pp. 35–44, 2015.
- [25] N. Suzuki, M. Ito, and F. Yatsuyanagi, "Effects of rubber/filler interactions on deformation behavior of silica filled SBR systems," *Polymer*, vol. 46, no. 1, pp. 193–201, 2005.
- [26] Y. Bai, S. Zhao, Y. Tong, X. Zhang, X. Liu, and M. Tian, "Study on the structure, morphology, and properties of end-functionalized star-shaped solution-polymerized styrene-butadiene rubber," *Journal of Applied Polymer Science*, vol. 128, no. 4, pp. 2516–2524, 2013.
- [27] M. Hassanabadi, M. Najafi, G. Hashemi Motlagh, and S. Saeedi Garakani, "Synthesis and characterization of end-functionalized solution polymerized styrene-butadiene rubber and study the impact of silica dispersion improvement on the wear behavior of the composite," *Polymer Testing*, vol. 85, article 106431, 2020.
- [28] H. Kondo, "Evaluation of rubber processing for unvulcanized rubber," *Nippon Gomu Kyokaishi*, vol. 87, no. 1, pp. 16–21, 2014.
- [29] S.-S. Choi, H.-M. Kwon, Y. Kim, E. Ko, and E. Kim, "Determination of bound rubber composition of filled SBR/BR blend compounds by analysis of the unbound rubber composition and bound rubber content," *Polymer Testing*, vol. 59, pp. 414–422, 2017.
- [30] C. Sangwichien, P. Sumanatrakool, and O. Patarapaiboolchai, "Effect of filler loading on curing characteristics and mechanical properties of thermoplastic vulcanizate," *Chiang Mai Journal of Science*, vol. 35, pp. 141–149, 2008.
- [31] J. M. Arguello and A. Santos, "Hardness and compression resistance of natural rubber and synthetic rubber mixtures," *Journal of Physics Conference Series*, vol. 687, no. 1, article 012088, 2016.
- [32] P. Sae-Oui, U. Thepsuwan, P. Thaptong, and C. Sirisinha, "Comparison of reinforcing efficiency of carbon black, conductive carbon black, and carbon nanotube in natural rubber," *Advances in Polymer Technology*, vol. 33, no. 4, 2014.
- [33] I. M. Ulfah, R. Fidyarningsih, S. Rahayu et al., "Influence of carbon black and silica filler on the rheological and mechanical properties of natural rubber compound," *Procedia Chemistry*, vol. 16, pp. 258–264, 2015.
- [34] A. F. Halasa, J. Prentis, B. Hsu, and C. Jasiunas, "High vinyl high styrene solution SBR," *Polymer*, vol. 46, no. 12, pp. 4166–4174, 2005.
- [35] A. Nakajima, K. Komuro, A. Ueda, H. Watanabe, and S. Akita, "Structure and physical properties of high-vinyl polybutadiene rubbers and their blends," *Pure and Applied Chemistry*, vol. 58, no. 12, pp. 1697–1706, 1986.
- [36] X. Liu and S. Zhao, "Study on structure and properties of SSBR/SiO₂ co-coagulated rubber and SSBR filled with nanosilica composites," *Journal of Applied Polymer Science*, vol. 109, no. 6, pp. 3900–3907, 2008.
- [37] P. K. Pal and S. K. De, "Effect of reinforcing silica on vulcanization, network structure, and technical properties of natural rubber," *Rubber Chemistry and Technology*, vol. 55, no. 5, pp. 1370–1388, 1982.
- [38] K. E. Polmanteer and C. W. Lentz, "Reinforcement studies—effect of silica structure on properties and crosslink density," *Rubber Chemistry and Technology*, vol. 48, no. 5, pp. 795–809, 1975.